The Journal of Engineering Geology, Vol.20, No.1, March, 2010, pp. 47-60

Hybrid Analysis of Displacement Behavior and Numerical Simulation on Tunnel Design

Yun-Young Jeong[1], Heui-Soo Han[2]*, and Jae-Ho Lee[3]

[1]Member, Senior Engineer and Doctor, Tunnel Division, Chungsuk Eng.Co., Seoul, Korea
[2]Member, Associate Professor, Dept. of Civil Engineering, Kumoh National of Technology, Gumi, Korea
[3]Member, Post Doctoral Researcher, School of Architecture & Civil Engineering, Kyungpook National University, Daegu, Korea

터널 변위 거동 및 수치 모의실험의 결합 해석

정윤영[1] · 한희수[2]* · 이재호[3]

[1]청석엔지니어링, [2]금오공과대학교 토목공학과, [3](주) 메카지오텍

This study is focused on the analysis of tunnel behavior to estimate the stability on tunnel design. An estimation method was proposed as a hybrid consideration, which contains the displacement analysis by 3D numerical simulation, the maximum displacement obtained after field measurement, and an assessment of tunnel stability using a deformation analysis proposed by Sakurai(1988, 1997). The points of case study by Sakurai(1988, 1997) were replotted considering his analysis. From the new analysis of the tunnel case study, the trend line for analyzed points is analogized, which curve is divided into stable, unstable and failure zone. To evaluate the estimation method, a special shape of railway tunnel was selected, which are the Inchon international airport rail way connected to subway line 9 in Gimpo, Korea. The point s of upper and below track on the Inchon international airport rail way were satisfied to the stability of tunnel after reinforcing. Also the points shows the higher apparent Young's modulus, which resulted from improvement on shear strength by the micro silica grouting and the supporting of umbrella method. Therefore, if new analysis used, proper tunnel reinforcing method could be selected according to tunnel strain and geological property.

Key Words : Tunnel deformation, Hybrid analysis, Sakurai's case study, Critical strain, Apparent young's modulus

이 연구는 터널설계의 안정성을 예측하기 위한 터널거동분석에 초점을 맞춘 것이다. 3차원 수치해석, 현장계측 후 최대변형 및 사쿠라이에 의해 제안된 터널변형에 관한 경험적 안정성 평가방법들을 결합한 평가기법을 사용하였다. 사쿠라이가 사용한 계측자료들은 새로운 해석기법을 도입하여 재해석되었다. 터널안정해석을 위한 사쿠라이의 경험적 추세선은 이론적 추세선으로 새로이 도입되었으며, 이는 안정, 불안정 및 파괴영역으로 구분되었다. 터널 현장자료의 새 해석기법을 평가하기 위한 현장의 적용 예로, 김포의 지하철 9호선으로 연결되는 인천공항의 지하철터널을 이용하였다. 그 결과 터널보강 후 인천공항 지하철의 상부 및 하부터널 모두 충분한 안정성을 보였다. 마이크로 실리카 그라우팅과 엄브레라방법에 의한 지반보강 후 겉보기 영계수가 상당히 증가하는 것을 볼 수 있었다. 그러므로, 제안된 새 해석기법을 이용하면, 터널변형과 지반조건에 따른 최적의 보강기법 선정에 활용할 수 있다.

주요어 : 터널변형, 결합해석, 사례연구, 한계변형율, 겉보기 탄성계수

Introduction

The stability control under tunnel construction deeply relates on displacement behavior of rock mass, estimation for the final values of displacement convergence after two to three times of tunnel width advance. Tunnel

*Corresponding author: hanhs@kumoh.ac.kr

design before underground excavation should be based on the assumption of displacement behavior estimated from similar geological condition because of data absence on field measurement at arch crown and surface subsidence. Measurement data gathered during the construction work in many fields have some problems, which the first measurement is usually obtained after a lot of initial displacement of surrounding rock mass occurred, and so displacement development does not contain preliminary displacement before excavation and initial one immediately after excavation. Tunnel survey has generally focused on the estimation of the maximum displacements in tunnel arch and crown as like the estimation studies of final deformation from the initial displacement (Song et al., 2002; Chung et al., 1993).

This paper is focused on a rational estimation of displacement behavior about tunnel stability in tunnel design. An estimation method was proposed as a hybrid consideration of three parts - the first is displacement development obtained by 3D numerical simulation before and after a cut face reaches to measurement points on arch crown, the second is the maximum displacement from field measurement on tunnel excavation, the third is an assessment of tunnel stability using a deformation analysis which the critical strain and apparent young's modulus proposed by Sakurai (1981, 1988, 1990, 1997) is estimated by the functional relationship between two parameters.

The key points of the hybrid consideration were that tunnel deformation was defined as the sum of the initial displacement estimated from 3D numerical simulation and the maximum displacement from field measurement, the tunnel deformation was investigated in the point of the tunnel stability using the above deformation analysis.

For application of the above hybrid consideration on tunnel design, it was selected the section closed to the base pile of Gimpo airport cargo building with some different shape for the connection between Inchon international airport railway and subway line 9. It was found that the above estimation method could be another useful indicator in preliminary plan usually supported by numerical calculation, if there were database of construction and geological condition.

Tunnel Design

Tunnel Sections

For tunnel sections of Inchon international airport railway contacting with Seoul subway line 9, there are connection area around station facility, passing through underground of Gimpo airport cargo with variable sections as parallel track as line alignment shown in Fig. 1.

Upper and below tracks of Inchon international railway

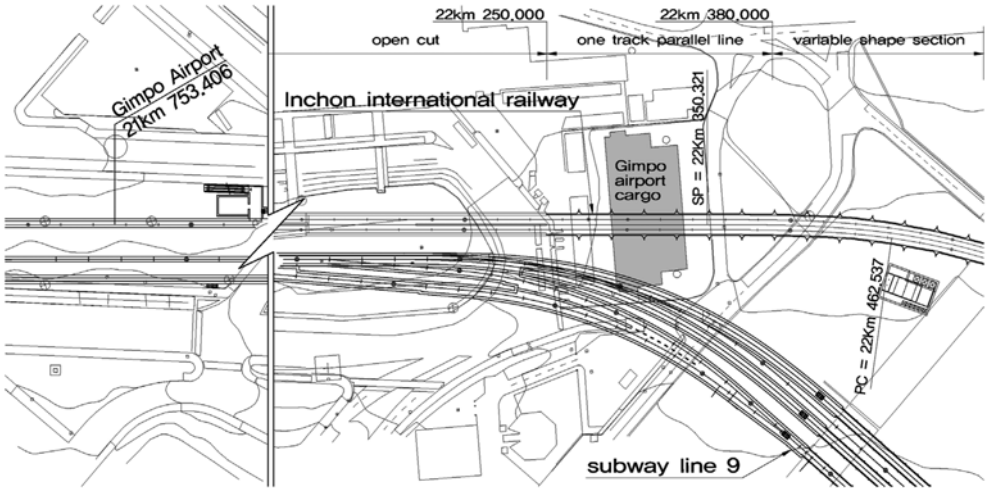

Fig. 1. Scheme of the study tunnel.

Table 1. Engineering properties of rock mass rating.

Parameters	Rating				
	I	II	III	IV	V
Deformation modulus, E_m (GPa)	53.5	26.2	6.8	2.6	0.43~0.9
Poisson's ratio	0.2	0.23	0.25	0.27	0.29
Unit weight (g/cm^3)	2.7	2.6	2.5	2.5	2.4
Cohesion (MPa)	32.2	9.3	6.6	4.5	0.2~0.9
Friction (^{o})	45	41	37	35	33

around Gimpo airport cargo were crossed from weak rock with RQD range of 0~23% to hard rock with that of 35~100%. This rock mass geologically consisted of granite and gneiss, showed engineering properties as summarized in Table 1 through empirical equations from RMR, laboratory test and field hydraulic jack test. The sections under Gimpo airport cargo located in rock mass of IV or V rating.

Tunnel Shape

For passenger's convenience at the transfer between Inchon international railway and subway line 9, tunnel excavation had to be done to overcome the level difference of both railways. Upper track and below track had to be passed respectively at different level around Gimpo airport cargo as shown in Fig. 2. Upper track located in the very close distance of 1.7 m~1.9 m apart from the base pile of the cargo building.

Therefore, there were some kinds of shape in cross sections as denoted in Fig. 3. Left figure (a) of Fig. 3 is a typical shape for tunnel sections around the base pile of Gimpo airport cargo building, figure (b) and (c) of that is a shape of variable shape sections which one-track lane is translated to double-track lanes at the rail level of Inchon international railway.

One-track lane tunnel passing under Gimpo airport cargo had a horseshoe shape section of width 7.1 m, arch crown of below track was apart only 0.2 m from the left side at invert of upper track lane. From the level difference of the both tracks and the above closeness between the upper track and base pile of cargo building in weak rock, some kinds of ground support were needed. Micro silica grouting had firstly performed as injection radius of 7.0 m, injection depth of 20 m and injection angle of 20^o on boundary area around the arch crown of both tracks. Arch crown of tunnel was supported before excavation by umbrella method; c.t.c. 500 mm, diameter 800 mm of steel pipe. Therefore, after the preliminary supports by the micro silica grouting, the tunnel excavation had performed in turn according to the excavation schedules, which are supporting of the umbrella method, excavation of upper face, rock bolting and shotcrete, excavation of below face, concrete lining on the below track lane. And then the above same schedules on the upper track lane had done as denoted in Fig. 4.

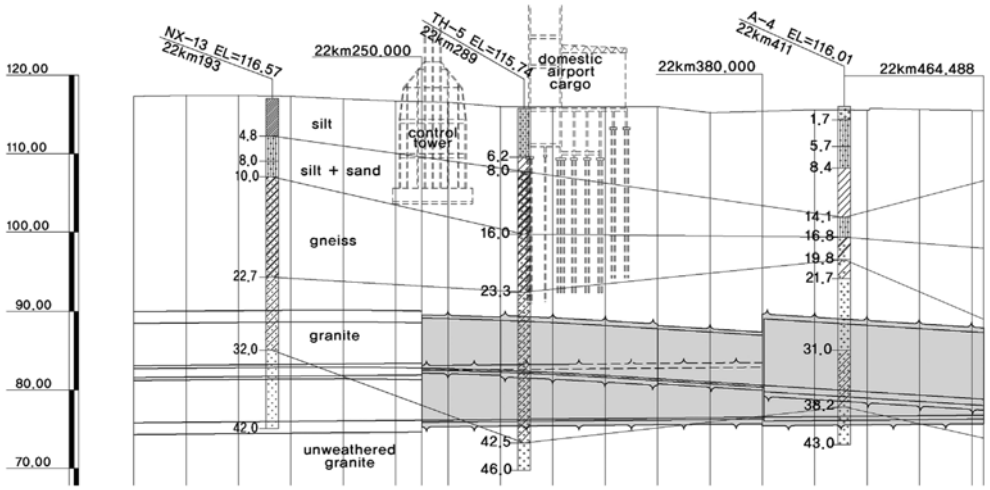

Fig. 2. Cross cut of the study tunnel sections.

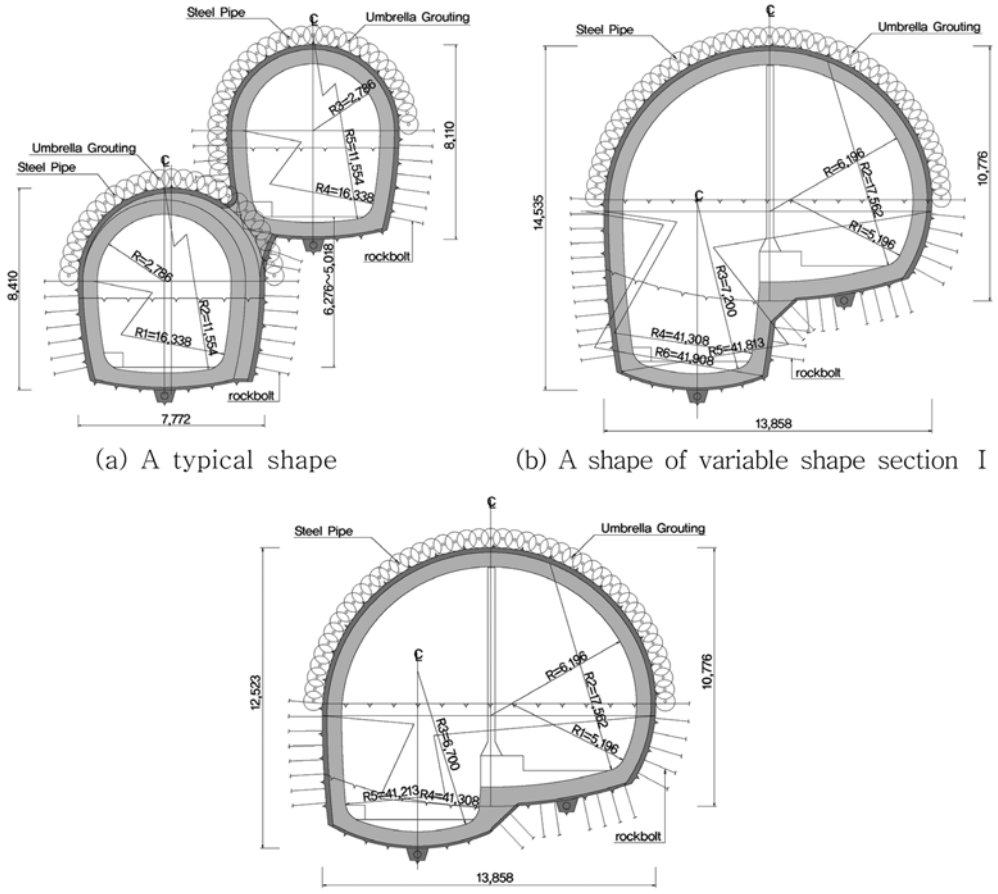

Fig. 3. Shape types of cross sections.

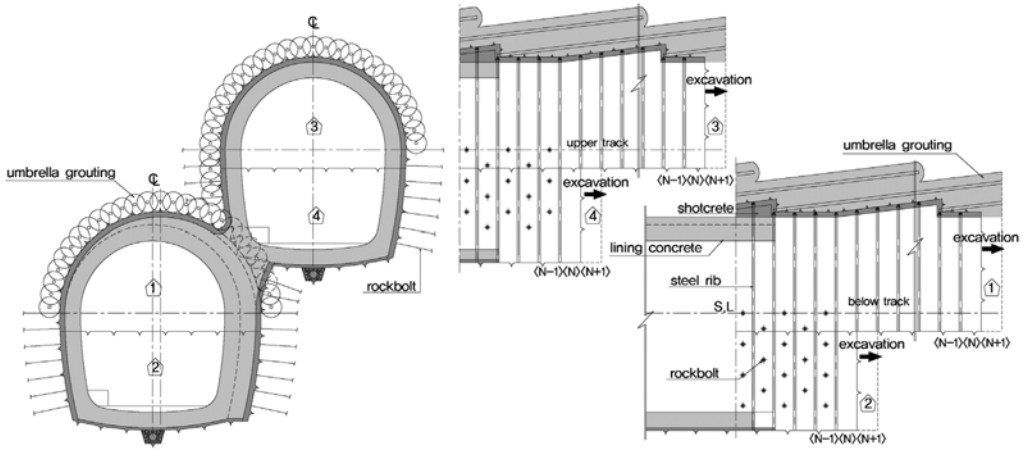

Fig. 4. Construction flow on one-track lane tunnel.

Relating to the stability of one-track lane tunnel under Gimpo airport cargo, survey work focused on the tunnel deformation during construction.

Tunnel Survey

Survey Plan

Tunnel deformation was recently estimated for crown settlements and displacement from tunnel wall at five measurement points on each track as denoted in Fig. 5 during two months. This measurement was performed in the interval of 20 m according to tunnel excavation. Two cross sections under Gimpo airport cargo and that around the cargo were needed to be monitored for stability of tunnel excavation. Weekly measurement was carried out by convergence tape extensometer as the record denoted in Table 2 about a cross section at 22 km260 of upper track lane. Performance criteria in Table 2 was a reasonable scale if it was compared with another abroad criteria summarized in Table 3.

Tunnel deformation

Tunnel deformation could be analyzed by tunnel convergence described as in Fig. 6, which final displacement (D_{final}) of tunnel surface is defined as an equation (1).

$$D_{sinal} = D_p + C_o + D_m \quad (1)$$

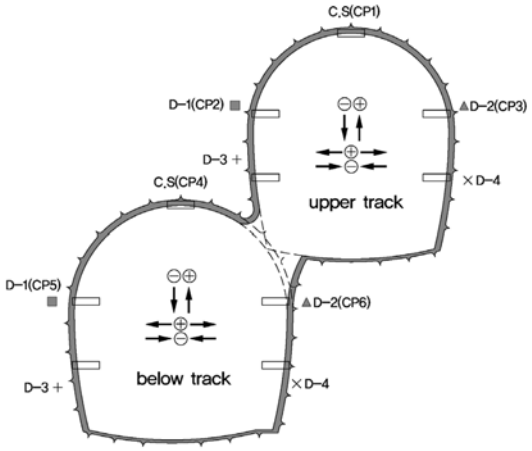

Fig. 5. Five measurement points on the both track lanes in a cross section.

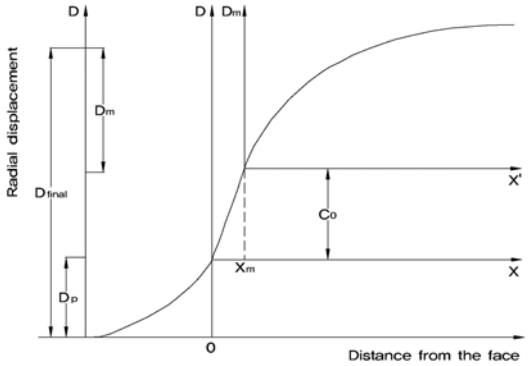

Fig. 6. Generalized form of tunnel convergence(Song et al., 2002; Chung et al., 1993).

Table 2. Sample record of weekly measurement in a cross section (22 km260) of upper track.

Data		Performance criteria (mm)				Measurement (mm)	
		Stable	Level I (warning)	Level II (daily check)		Ex-Check	Check
Crown settlement	O CS	under 5.23	~80	over 80	10mm/day	5.5	5.4
Displacement of tunnel wall	■ D-1	under 4.58	~50	over 50	10mm/day	5.7	5.9
	▲ D-2	under 4.58	~50	over 50	10mm/day	4.0	4.0
	+ D-3	under 4.58	~50	over 50	10mm/day	0.0	0.6
	× D-4	under 4.58	~50	over 50	10mm/day	0.0	1.2

Table 3. Abroad criteria about crown settlements and displacement inward (Chun et al, 1996).

Rock	Deformation modulus, (GPa)	Crown settlement (mm)			Displacement inward (mm)	
		Japanese			Austrian	Japanese
		Level I	Level II	Level III	3~4% of rockbolt length	One track line
Weathered rock	0.15	13.6	44.2	129.0	90.0~120	under 75.0
Weak rock	1.0	5.1	18.7	51.0	90.0~120	under 75.0

Where D_p is displacement until tunnel excavation approached to a cross section, C_o is displacement expected in the cross section on that tunnel excavation advanced to x distance over the section, this distance is needed to have the working space for measuring. And D_m is measured displacement by stress relaxing after displacement.

According to the tunnel measurement plan, displacement behaviors of four sections were monitored during two months. The maximum displacement of crown settlement and tunnel wall were measured respectively about upper track and below track as summarized in Table 4. And so the displacement of upper track was obtained after rock mass was some loosed by means of below track excavation before upper track excavation. It could be not appropriate for regression analysis about displacement behavior.

3D Numerical Ananlysis

Model

Tunnel sections under Gimpo airport cargo had geometrically unusual shape with the different level between upper track and below track as one track lane as described in Fig. 5. It was not sufficient to find out the interaction between both tracks that tunnel survey had progressively performed according to tunnel construction step in the certain period. 3D numerical computation was used for investigating not only the interaction between both tracks, but also the displacement (D_p) on the time that tunnel excavation approached to the measurement points. Model boundary was defined as the minimum area included four cross sections used for tunnel survey in chapter3. Simulation of tunnel excavation and support was executed under the same condition except micro silica grouting around the pile of cargo building as three dimensional model described in Fig. 7(a). The simulation results of the both tracks were analyzed according to the figure number shown in Fig. 7(b).

Simulation model had the properties of Mohr-Coulomb model resulted from Hoek-Brown parameters. The elastic stiffness of pre-reinforced zones by umbrella

Table 4. The maximum displacement of crown settlement and tunnel wall (D_m).

		Displacement (mm) of below track (sta. 22kmOOO)				Displacement (mm) of upper track (sta. 22kmOOO)			
		280	300	320	340	280	300	320	340
Crown ettlement	O CS	–2.8	–2.4	–1.5	–1.8	–5.8	–5.8	–5.5	–2.9
Displacement of tunnel wall	■ D-1	1.6	1.3	1.2	1.5	5.5	5.0	4.9	2.3
	▲ D-2	–1.8	–1.3	–2.3	–1.4	–4.3	–4.0	–3.8	–1.4
	+ D-3	0.4	0.2	1.2	0.9	2.1	-	-	-
	× D-4	0.4	0.6	1.4	1.2	2.8	-	-	1.9

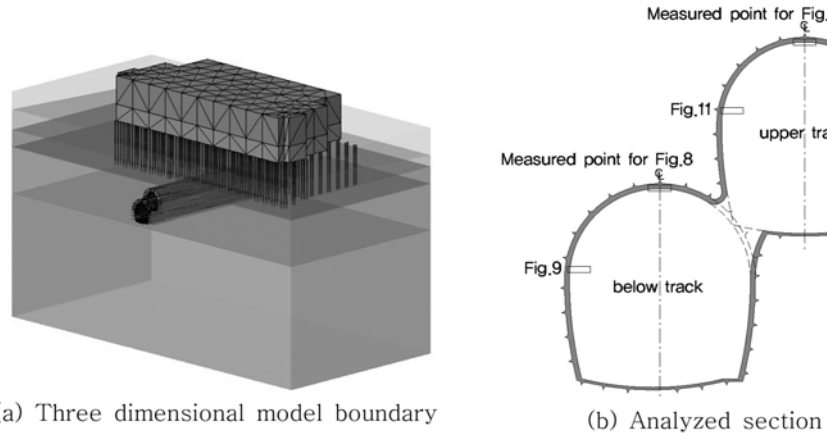

(a) Three dimensional model boundary (b) Analyzed section

Fig. 7. Model boundary and analyzed section in numerical simulation.

Table 5. Input data of the simulation.

Model elements	Deformation modulus E_m (GPa)	Cohesion (MPa)	Friction angle (°)	Unit. Weight (tf/m^3)
Silt	0.04	0.10	30	1.9
Silt + sand	0.43	0.20	32	2.3
Gneiss	0.90	0.90	33	2.4
Granite	2.60	4.50	35	2.5
Reinforced area	0.97	0.91	33	2.4

grouting (Song and Cho, 2006) and the geological data for ground resulted in the physical properties of Table 5 used as input data of this simulation.

Deformation behavior

Tunnel deformation obtained through the above simulation was analyzed as the deformation of crown and tunnel wall in the point of the interaction between two track lanes during tunnel construction. Fig. 8 shows deformation behavior in the crown (Cp4) of below track lane at Sta. 22 km300 and 22 km320 beneath the pile of the cargo building. It was found that previous displacement occurred respectively 1.57 mm and 1.60 mm until that tunnel excavation advanced to the cross section of Sta. 22 km300 and 22 km320. Crown settlement rapidly increased before and after tunnel excavation at the cross section, additional excavation of upper track induced the displacement increase of about 0.36 mm before tunnel excavation advanced to the same section of upper track.

Fig. 9 shows deformation behavior in the left wall (Cp5) of below track lane at Sta. 22 km300 and 22 km320. It

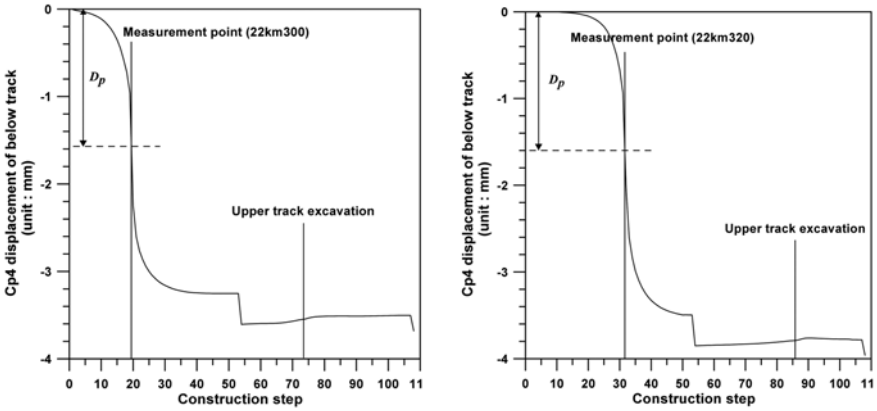

(a) Sta. 22km300 in Cp4 (b) Sta. 22km320 in Cp4

Fig. 8. Deformation behavior in Cp4 of below track at Sta. 22 km300 and 22 km320.

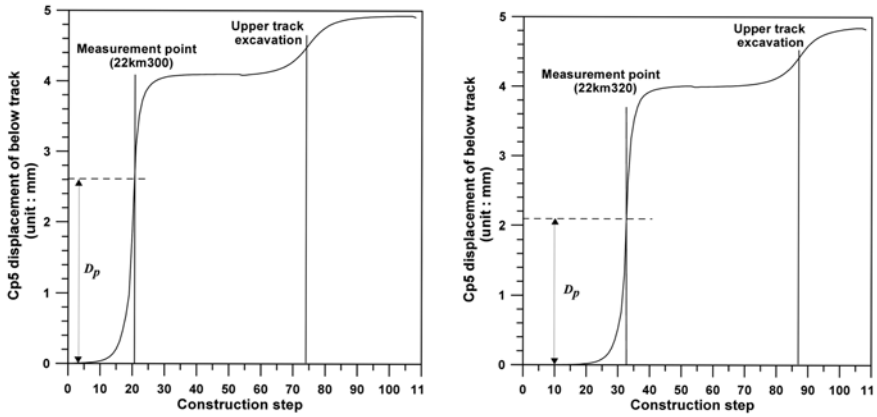

(a) Sta. 22km300 in Cp5 (b) Sta. 22km320 in Cp5

Fig. 9. Deformation behavior in Cp5 of below track at Sta. 22 km300 and 22 km320.

was found that previous displacement occurred respectively 2.61 mm and 2.09 mm until that tunnel excavation advanced to the cross section of Sta. 22 km300 and 22 km320. Displacement outwards of tunnel surface rapidly increased before and after tunnel excavation at the cross section, additional excavation of upper track induced the displacement increase of about 0.58 mm on that the excavation approached to the same section of upper track.

Fig. 10 shows deformation behavior in the crown (Cp1) of upper track lane at Sta. 22 km300 and 22 km320. It was firstly found that the tunnel excavation of below track until the construction step 54 induced the rock mass around the crown of upper track loosed. After previous displacement of about 1.8 mm was induced, crown settlement occurred respectively 2.75 mm and 2.93 mm until that tunnel excavation advanced to the cross section of Sta. 22 km300 and 22 km320. The settlement rapidly increased before and after tunnel excavation at the cross section, too.

Fig. 11 shows deformation behavior in the left wall (Cp2) of upper track lane at sta. 22 km300 and 22 km320. It was found that the tunnel excavation of below track caused a few of inverse deformation in rock mass around the left wall (Cp2) of upper track. Displacement outwards from tunnel surface occurred respectively 1.22 mm

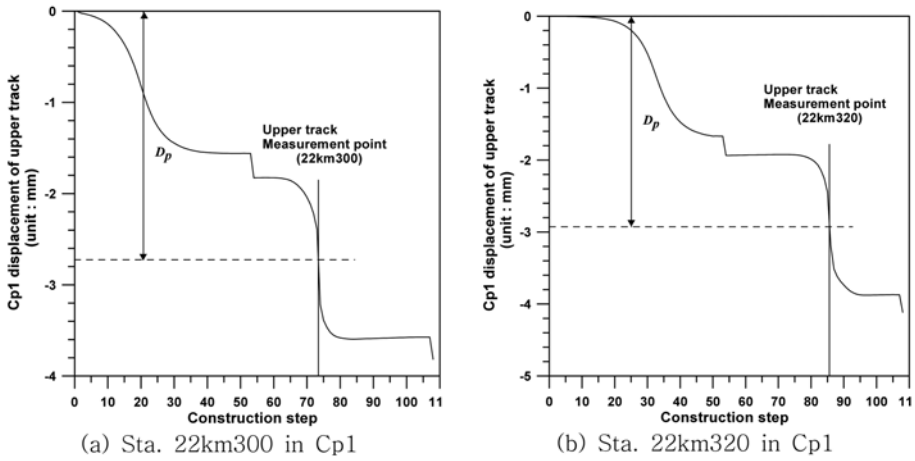

Fig. 10. Deformation in Cp1 of upper track at Sta. 22 km300 and 22 km320.

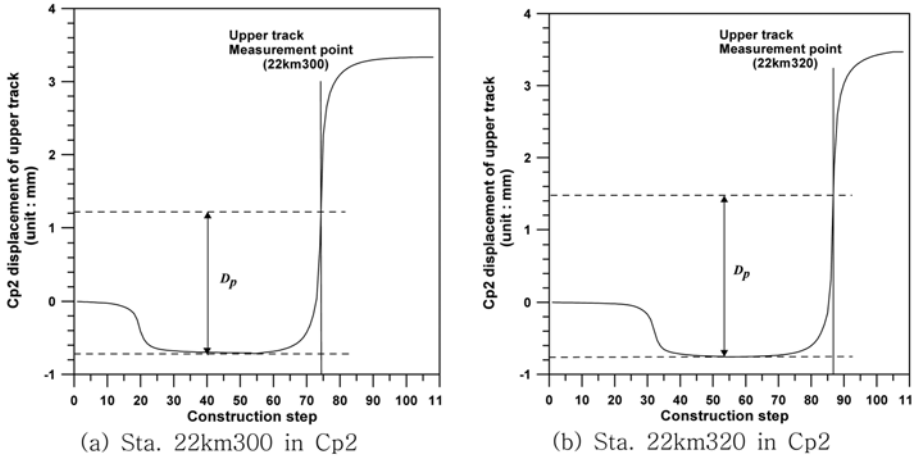

Fig. 11. Deformation in Cp2 of upper track at Sta. 22 km300 and 22 km320.

and 1.47 mm until that tunnel excavation advanced to the cross section of Sta. 22 km300 and 22 km320. The displacement rapidly increased before and after tunnel excavation at the cross section, too.

It was thought that the above simulation result proved the interaction between upper and below track during the tunnel construction. Previous deformation (C_a) in the arch crown and tunnel wall of both track lanes was summarized about the cross section of Sta. 22 km280, 22 km300, 22 km320, 22 km340 in Table 6. And then analyzed deformation (C_a) from the interaction between the both tracks was summarized in Table 7, for the case of upper track lane, that was estimated to be already included in the previous deformation.

Estimation of tunnel deformation, stability and support system

Estimation of the final deformation

Numerical computation suggested the estimation of the previous deformation and three dimensional behaviors by the interaction between both track lanes. In this paper, the final deformation (D_{final}) was defined as an equation (2).

$$D_{final} = D_p + C_a + D_m \quad (2)$$

Where (Table 6) is defined as the same denoted in an equation (1), (Table 7) is displacement analyzed from the interaction between upper and below track lanes, which is noted as in an equation (1), (Table 4) is the maximum value of the crown settlement and the displacement of tunnel wall resulted from the tunnel survey.

The final deformation of measurement point at both track lanes were summarized in Table 8 according to an equation (2).

Tunnel stability

Tunnel stability was decisively estimated and analyzed by two indicators which were based on the above final deformation, utilizing a critical strain and apparent Young's modulus of crown settlement and surface settlement (Sakurai, 1981; Sakurai, 1982; Sakurai, 1987).

Table 6. Previous deformation(D_p) In the arch crown and tunnel wall of both track lanes.

Measurement points		Previous deformation, (mm)			
		Sta. 22 km280	Sta. 22 km300	Sta. 22 km320	Sta. 22 km340
Upper track lane	Cp1	–3.34	–2.75	–2.93	–3.29
	Cp2	1.33	1.22	1.47	2.54
	Cp3	–2.77	–2.74	–2.77	–3.01
Below track lane	Cp4	–1.33	–1.57	–1.60	–2.38
	Cp5	2.12	2.61	2.09	2.85
	Cp6	–1.82	–2.97	–2.43	–3.03

Table 7. Analyzed deformation(C_a) in the arch crown and tunnel wall of both track lanes.

Measurement points		Analyzed deformation, (mm)			
		Sta. 22 km280	Sta. 22 km300	Sta. 22 km320	Sta. 22 km340
Upper track lane	Cp1	0	0	0	0
	Cp2	0	0	0	0
	Cp3	0	0	0	0
Below track lane	Cp4	–0.36	–0.35	–0.36	–0.36
	Cp5	0.80	0.60	0.57	0.73
	Cp6	0.43	0.40	0.37	0.30

Table 8. The final deformation of measurement points at both tracks.

Measurement points		Final deformation, (mm)			
		Sta. 22 km280	Sta. 22 km300	Sta. 22 km320	Sta. 22 km340
Upper track	Cp1	–9.14	–8.55	–8.43	–6.19
	Cp2	6.83	6.22	6.37	4.84
	Cp3	–7.07	–6.74	–6.57	–4.41
Below track	Cp4	–4.49	–4.32	–3.46	–4.54
	Cp5	4.52	4.51	3.86	5.08
	Cp6	–3.19	–3.87	–4.36	–4.03

The strain (ε_θ) was simply defined at the crown settlement as the proportion of settlement extent (U_c) to the tunnel radius (α) as an equation (3).

$$\varepsilon_\theta = \frac{U_c}{\alpha} \times 100 \quad (3)$$

From elastic circular opening problem (Timoshenko and Goodier, 1970) and tunnel stability in terms of strain and apparent Young's modulus (Sakurai, 1988; Sakurai, 1990), apparent Young's modulus of crown settlement

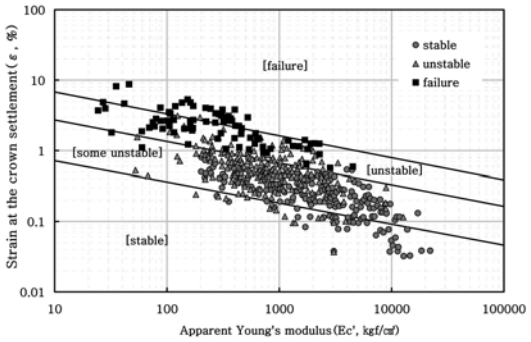

Fig. 12. Case studies about critical strain and apparent Young's modulus estimation.

means the modulus respectively defined in equation (4).

$$E_c' = \frac{(1-\nu^2)\bullet\alpha\bullet\omega\bullet H}{U_c}\left\{2K_o' - \frac{(1-2\nu)}{(1-\nu)}\right\} \quad (4)$$

Where E_c' is apparent Young's modulus about the crown settlement, U_c is the measurement value of the crown settlement and displacement from tunnel wall, ω is unit weight, H is overburden height, α is the radius of tunnel, ν is Poisson' ratio and K_o' is initial stress ratio. Sakurai showed the level into four stages in relation of strain and apparent Young's modulus estimation to the degree of tunnel stability as shown in Fig. 12.

From equation (3) and (4), apparent Young's modulus could be rearranged as equation (5).

$$E_c' = \frac{100}{\varepsilon_\theta}(1-\nu^2)\bullet\omega\bullet H\left\{2K_o' - \frac{(1-2\nu)}{(1-\nu)}\right\} = \frac{f(\alpha)}{\varepsilon_\theta} \quad (5)$$

By equation (5), it proves that stress function, $f(\alpha)$, is dependent of unit weight ω, overburden height H, Poisson' ratio ν, and initial stress ratio K_0'. And, the stress function $f(\alpha)$ could be fixed as stress condition in tunneling construction, and strain can ε_θ be determined by measured deflection of crown in downward direction/ radius of Tunnel. Deformation of rock or soil sample can be obtained by the equation $\sigma = E\bullet\varepsilon$, and Young's modulus E, and strain can be established as inverse proportion relationship.

From the stress-strain curve, the deformation levels of tunnel are classified into three layers as elasticity, transition and plasticity zone as shown in Fig. 13.

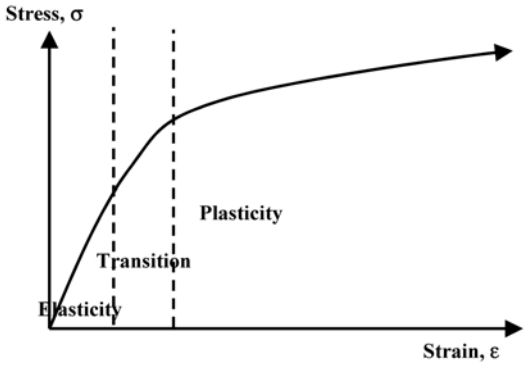

Fig. 13. Stress and strain curve in deformation of soil and rock sample.

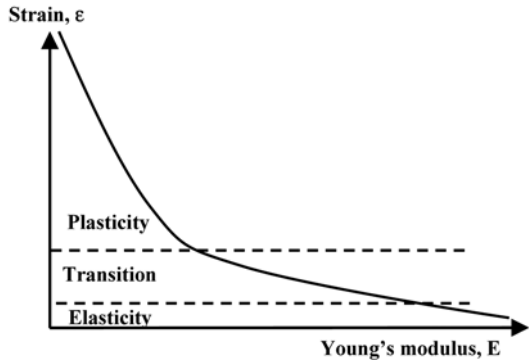

Fig. 14. Theoretical curve of strain and Young's modulus in soil and rock deformation.

Furthermore, the relation of Young's modulus E, andstrain ε, may be plotted by theoretical curves as shown in Fig. 14. From Fig. 14 and equation (5), it is proved that the relation between the strain and Young's modulus could be used as indicators of tunnel behaviors.

Fig. 15 (a) shows the curve of apparent Young's modulus E' and strain ε that can be divided into stable, unstable and failure zone according to the Sakurai's case study. It is suggested that to set up each layer, the dotted tangent line of stable layer is extended to the Y-axis, after that the other dotted line is drawn vertically again. Two dotted lines make the three divided layer, which are failure, unstable, and stable layer. If tunnel reinforcing methods are applied, the points representing of tunnel deformation and strength would move to the right from left because of the rock stiffness increasing as shown in Fig. 15(a). The points of case study by Sakurai can be re-plotted as

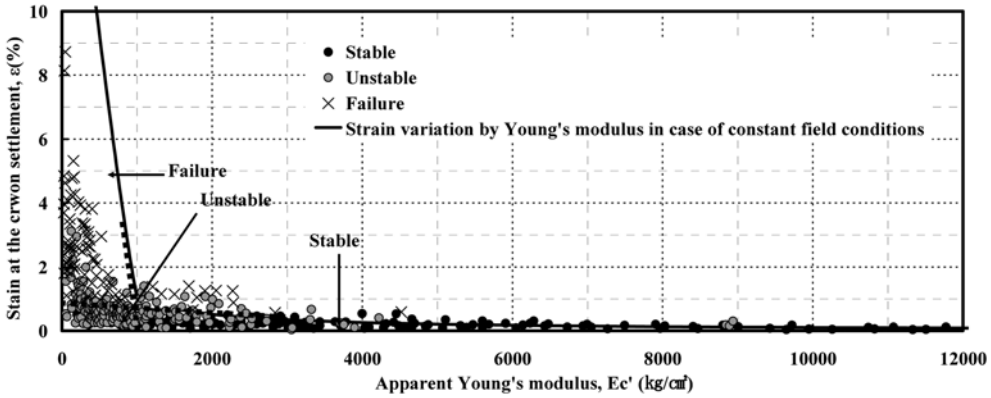

(a) Simple realtionship curve between strain and apparent Young's modulus for tunnel stavility estimation

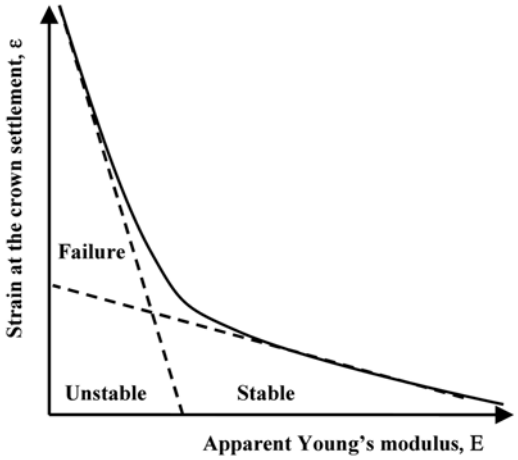

(b) Graph of strain and apparent Young's modulus in Sakurai's case study (1988, 1990) and equation (5)

Fig. 15. Hazard warning levels using the relationship of strain and apparent Young's modulus in tunnel problem.

shown in Fig. 15(b) considering Fig. 15(a). It is observed that where are large and small, there were no problem in the tunnel because of high stiffness of rock. Whereas tunneling problems were encountered where is small and large. And if apparent Young's modulus is fixed, tunnel stability is dependent by strain at tunnel crown settlement.

From the new analysis of Sakurai's case study, the trend line for analyzed points is analogized, which curve is almost connecting the upper points of Fig. 15(b). The curve is adjusted to have following equation (6).

$$\varepsilon_\theta = \frac{1500}{E_c'} \tag{6}$$

As you can see, most of failure points are located in failure zone; also the same phenomena are shown for unstable and stable points in Fig. 15(b)

Fig. 16 showed the relation resulted from the above one-track lanes around the Gimpo airport cargo about the crown settlement for tunneling condition with the final deformation and the parameters respectively summarized in Table 8 and Table 9. The points appeared in Fig. 16 indicates the stability of tunnel deformation of upper and below track after reinforcing. The points in Fig. 16 shows the apparent Young's modulus within the stable zone, which resulted from improvement on

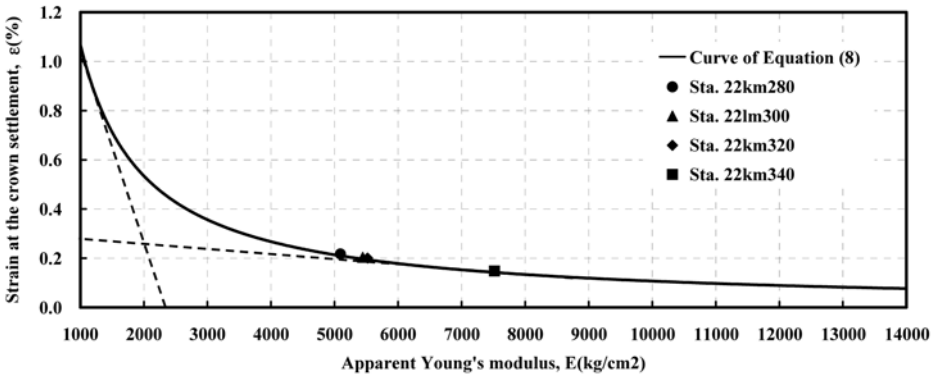

(a) Upper track

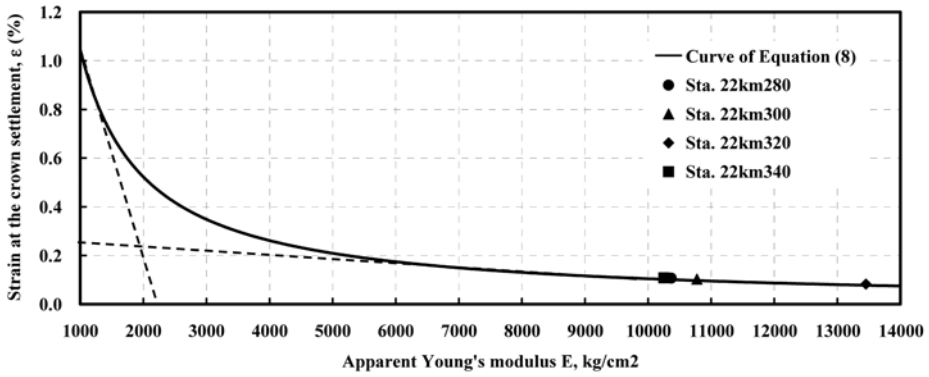

(a) Below track

Fig. 16. Stability estimation about tunneling around the airport cargo.

Table 9. Parameters related to apparent Young's modulus estimation.

Parameters	Upper track	Below track
Overburden height (H)	27.7 m	36.5 m
Tunnel radius (α)	4.2 m	4.2 m
Unit. Weight (ω)	2.4 KN/m^3	2.4 KN/m^3
Poisson's ratio (ν)	0.32	0.32
Initial stress ratio (K_o')	1.2	1.0

shear strength by the micro silica grouting and the supporting of umbrella method.

Effectiveness evaluation of tunnel support system

Evaluation of Tunnel support system is estimated in equation (7) as the support effectiveness (E_{sfs}) about the surface settlement (S_S') of the first floor of the Gimpo airport cargo and the ground condition improved by the micro silica grouting and the supporting of umbrella method. Equation (8) showed the support effectiveness (E_{sfs}) of crown settlement in Tunnel support system.

$$E_{sfs}=\frac{E_S'}{E} \tag{7}$$

$$E_{sfs}=\frac{E_c'}{E} \tag{8}$$

Where E_s' is apparent Young's modulus of the surface settlement, deformation modulus according to the ground condition, means apparent Young's modulus defined in equation (4).

And then the apparent Young's modulus of surface settlement , is defined as the follows;

Table 10. Parameters related to the support effectiveness in surface settlement.

Parameters	Data summary
Overburden height (H)	27.7 m
Tunnel diameter (d)	8.4 m
Unit. Weight (ω)	2.4 KN/m^3
Poisson's ratio (ν)	0.32
Deformation value (E)	0.97 GPa (weak rock improved by grouting) 0.43 GPa (weathered rock)
Settlement of the first floor (S_s')	2.047 mm

Table 11. Results of the support effectiveness about crown settlement in tunnel.

		Sta. 22 km280	Sta. 22 km300	Sta. 22 km320	Sta. 22 km340
Upper track	Apparent Young's modulus (GPa), E_c'	0.509	0.544	0.552	0.752
	Ratio of support effectiveness, E_{sfc}	1.180	1.270	1.28	1.750
Below track	Apparent Young's modulus (GPa), E_c'	1.037	1.077	1.345	1.025
	Ratio of support effectiveness, E_{sfc}	1.150	1.200	1.50	1.140

$$E_s' = \frac{(1-\nu^2)\bullet\omega\bullet H}{S_s'} \times \frac{4d^2H}{H^2-d^2} \tag{9}$$

Where E_s' is apparent Young's modulus about the surface settlement, S_s' is the measurement value of the surface settlement, ω is unit weight, H is overburden height, d is the diameter of tunnel, ν is Poisson' ratio and K_o' is initial stress ratio. Table 10 show the parameters related to find the support effectiveness about surface and crown settlement. It was found that E_{sfs} was 3.3, E_{sfs} about upper track was 1.18~1.75, and E_{sfs} about below track was 1.14~1.5 through equation (8), (9) and Table 10. In this result, the tunnel deformation investigated in this paper was certainly stable and the support system effective as indicated in Fig. 16 and Table 11.

Conclusion

In tunnel sections of Inchon international airport railway contacting with Seoul subway line9, tunnel survey has been recently performed during the tunnel construction. The section around the Gimpo airport cargo was one track parallel lane with the level difference between upper and below tracks, the crown displacement and the displacement in tunnel wall was measured during about two months according to the construction steps. The result of displacement measurements was not clear to find the previous deformation(D_p) and the interaction between both lanes, which they were supported by numerical simulation of three dimensional modeling. This paper focused on a rational estimation of displacement behavior about tunnel stability in tunnel design. An estimation method was proposed as a 3D numerical simulation, the prediction of maximum displacement from field measurement on tunnel excavation, an assessment of tunnel stability using deformation analysis through the critical strain and apparent young's modulus.

The results are summarized as follows;

1) The final deformation of tunnel section was estimated in this paper by the previous deformation, the interaction between both lanes defined from numerical modeling, and the maximum displacement during tunnel survey.

2) It is suggested that simple estimation method of tunnel stability can be used by Young's modulus and measured strain data of tunnel, which is the revised method from the Sakurai's case study. In the method, tunnel stability is divided into three sections, stable, unstable and failure zone from the curve of strain and Young's modulus. From case study of tunnel stability, the analyzed points of both upper and low tunnel are placed in stable zone.

3) As the newly suggested tunnel stability analysis from the Sakurai's case study, the study of tunnel behavior was carried out through two indicators which are the critical strain of tunnel deformation and apparent Young's modulus of rock stiffness. Therefore, from new analysis, proper tunnel reinforcing method could be selected according to the measured tunnel deformation and in-situ geological property.

4) It was consequently found that the crown settlement of both lanes was in respectively stable layer, umbrella method and micro silica grouting were suitable for tunnel support in the point of this tunnel reinforcing.

References

Chun, B.S., Lee, M.G., Nam, S.S. and Shin, G.S., 1996, A case study on the displacement behavior of the subway NATM, Proc. KGS Spring 96 National Conference, Seoul, 183-204(Korean).

Chung, H.J., Cho, K.T., Kim, T.Y. and Kim, Y.I., 1993, A case study on displacement forecasting method in tunneling by NATM in urban area, Proc. KGS Spring 93 National Conference, Seoul, 27-32(Korean).

Sakurai, S., 1981, Direct strain evaluation technique in construction of underground openings, Proc. 22nd US Symp. Rock Mech., Cambridge, Massachusetts, M.I.T., 278-282.

Sakurai, S., 1982, An evaluation technique of displacement measurements in tunnels, J. of Geotechnical and Engineering, JCSE, Vol. 317, 93-100.

Sakurai, S., 1988, Back analysis of measured displacement in a shallow tunnel excavated in sandy materials, International Symposium on Underground Engineering, Editor B. Singh, 14-17 April, New Delhi, India, Vol. 1, 33-42

Sakurai, S., 1990, Monitoring the stability of cut slopes, Proc. Mine Panning and Equipment Selection, Calgary, Balkema, Editor Singhal & Vavra, 269-274.

Sakurai, S., 1997, Lessons learned from field measurements in tunneling, Tunnelling and Underground Space Technology, Vol. 12, 453-460.

Song, S.G., Yang, H.S. Lim, S.S. and Chung, S.K., 2002, Estimation of final deformation of hard rock tunnel using early measured deformation, Tunnel & Underground, Vol. 12, 99-106.

Song, K.I. and Cho, G.C., 2006, Equivalent design parameter determination for effective numerical modeling of pre-reinforced zones in tunnel, Tunnelling Technology, Vol. 8, 151-163(Korean).

Timoshenko, S. and Goodier, J., 1970, Theory of Elasticity, McGraw-Hill, New York, 567p.

2010년 2월 5일 원고접수, 2010년 3월 12일 게재승인

정윤영
청석엔지니어링
138-802, 서울특별시 송파구 가락동 57번지 청석B/D
Tel: 02)405-0182
Fax: 02)405-0149
E-mail: yyjeong@cse.co.kr

한희수
금오공과대학교 토목공학과
730-701, 경상북도 구미시 양호동 1번지
Tel: 054)478-7618
Fax: 054)478-7629
E-mail: hanhs@kumoh.ac.kr

이재호
(주)메카지오텍
706-821, 대구광역시 수성구 범어동 200-10번지
Tel: 053)743-6776
Fax: 053)743-6772
E-mail: mecageotech@naver.com